Chapter 3

Hyperpolarizabilities of Push−Pull Polyenes

Molecular Orbital and Valence-Bond Charge-Transfer Models

J. W. Perry[1,2], S. R. Marder[1,2], F. Meyers[2,3], D. Lu[2], G. Chen[2], W. A. Goddard, III[2], J. L. Brédas[3], and B. M. Pierce[4]

[1]Jet Propulsion Laboratory, California Institute of Technology, Pasadena, CA 91109
[2]Beckman Institute, California Institute of Technology, Pasadena, CA 91125
[3]Center for Research on Molecular Electronics and Photonics, Université de Mons-Hainaut, Place du Parc 20, B-7000 Mons, Belgium
[4]Hughes Aircraft Company, Radar Systems, Building R2, MS, V518, P.O. Box 92426, Los Angeles, CA 90009−2426

In this paper we review two theoretical approaches that illustrate the relationships between molecular (hyper)polarizabilities and bond-length alternation (*BLA*). In one approach, we employ sum-over-states calculations at the INDO-SDCI level on $(CH_3)_2N-(CH=CH)_4-CHO$, including an external, static, homogeneous electric field that tunes the degree of ground-state polarization and *BLA*. In the second approach, we use a simple semiclassical model, wherein the mixing of valence bond (VB) and charge-transfer (CT) states along a *BLA* coordinate is treated. Qualitatively, the two approaches give very similar structure-property trends, that are consistent with experimental hyperpolarizability data on donor-acceptor polyenes. The agreement of the calculated trends reflects the importance of VB-CT energetics in determining them.

Recent experimental work has demonstrated a correlation between the bond length alternation and the first and second hyperpolarizabilities (β and γ) of donor-acceptor (DA) substituted (push-pull) polyenes (*1, 2*). The bond length alternation, *BLA*, in DA polyenes is defined as the average of the difference in the length between adjacent carbon-carbon bonds in the polymethine, $(CH)_n$, chain. The structure of such molecules can be understood qualitatively as resulting from a superposition of valence-bond (VB) and charge-transfer (CT) limiting resonance structures (Figure 1). Experimentally, molecules have been examined where *BLA* was varied from the polyene limit of ~-0.1Å to values approaching the opposite *BLA* limit of ~0.1Å, by use of acceptors of varying strength and groups that gain aromaticity on polarization for coarse tuning. Additionally, the structures have been fine tuned by the use of solvents of varying polarity. It was shown that $\mu\beta$ (*2*) and γ (*1, 3*) exhibit positive

and negative peaks and sign changes as the ground-state polarization is increased, with *BLA* varying concomitantly from -0.12 towards 0.12Å. These experimental trends are consistent with those calculated with a finite-field AM-1 molecular orbital method, described previously (*4*). In this paper, we provide an overview of recent work, presented in part at the 1994 fall American Chemical Society meeting in Washington, DC, on detailed sum-over-states molecular orbital calculations (*5, 6*) at the intermediate neglect of differential overlap level (including configuration interaction with single and double excitations, INDO-SDCI) and a semiclassical valence-bond/charge-transfer (VB-CT) model (*7, 8*) that elucidate the relationships between *BLA*, the related π-bond order alternation, *BOA*, (*vide infra*) and α, β and γ.

Relationships between *BOA* and α, β, and γ at the INDO-SDCI level

In order to correlate α, β, and γ with geometric and electronic structure, we examined, at the semi-empirical INDO level, the molecule $(CH_3)_2N$-$(CH=CH)_4$-CHO (Figure 1) in the presence of a static, homogeneous electric field. Fields of high strength were used to tune the degree of ground-state polarization, *BLA* and the related parameter, *BOA* (Figure 2). The molecular polarizabilities were evaluated using a sum-over-states approach in combination with INDO-SDCI calculations (*5, 6*). These calculations allowed us to identify the electronically excited states that play an important role in the nonlinear optical response (*5, 6*). The correlation of the polarizabilities with *BOA* is shown in Figures 3-5 (note that ground-state polarization increases concomitantly with BOA). In addition, this analysis allowed us to compare the values of the polarizabilities obtained from the full sum-over-states expressions for α_{sos}, β_{sos} and γ_{sos} and simplified two or multilevel level models in which:

$$\alpha_{model} \quad \propto \quad \frac{\mu_{ge}^2}{E_{ge}} \tag{1}$$

$$\beta_{model} \quad \propto \quad \frac{\mu_{ge}^2(\mu_{ee}-\mu_{gg})}{E_{ge}^2} \tag{2}$$

$$\gamma_{model} \quad \propto \quad -\underbrace{\left(\frac{\mu_{ge}^4}{E_{ge}^3}\right)}_{N} + \underbrace{\sum_{e'}\left(\frac{\mu_{ge}^2\,\mu_{ge'}^2}{E_{ge}^2\,E_{ge'}}\right)}_{T} + \underbrace{\left(\frac{\mu_{ge}^2(\mu_{ee}-\mu_{gg})^2}{E_{ge}^3}\right)}_{D} \tag{3}$$

where μ and E are the dipole matrix element and transition energy, respectively, between the subscripted states. The subscripts g, e, and e' label the ground, first excited and upper excited states, respectively.

The first-order polarizability, α, exhibits a peak at zero *BOA* (referred to here as the cyanine limit) (Figure 3). In the two-level model expression (eq. 1) α is dependent on two factors, $(1/E_{ge})$ and μ_{ge}^2. As can be seen in Figure 3 there is a very good correlation between the converged sum-over-states calculation (30 states) and that of the two level model. Examination of the dependence of $(1/E_{ge})$ and μ_{ge}^2 on *BOA* reveal that they both peak near the cyanine-limit (Figure 3), thus providing insight into the dependence of α on *BOA*.
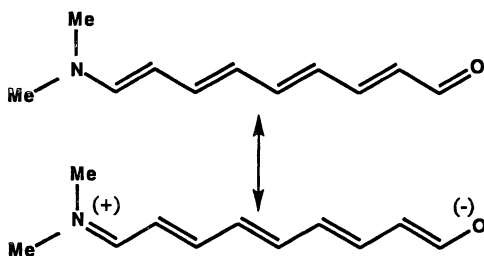
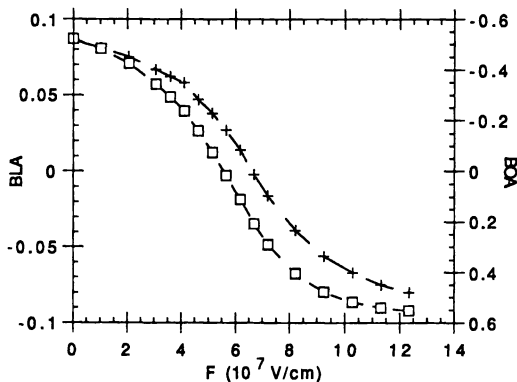Figure 1. Valence-bond and charge-separated resonance structures for $(CH_3)_2N-(CH=CH)_4-CHO$.

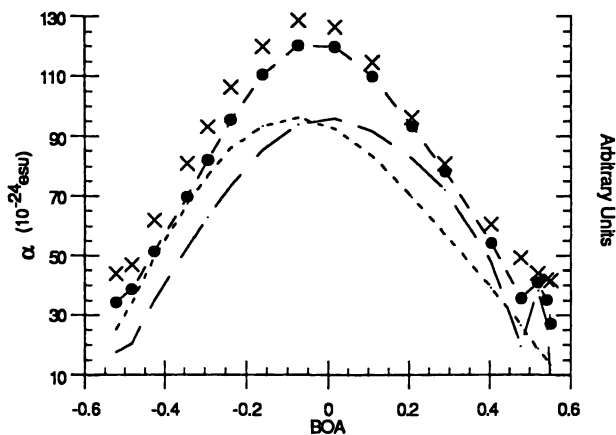Figure 2. Evolution of *BLA* and *BOA* vs. applied field (F) for $(CH_3)_2N-(CH=CH)_4-CHO$.

Figure 3. Evolution of: α_{sos} (crosses) and α_{model} (full circles, dashed line) in 10^{-24} esu; $1/E_{ge}$ (short dashed line) and μ_{ge} (long dashed line) in arbitrary units, plotted vs. BOA.
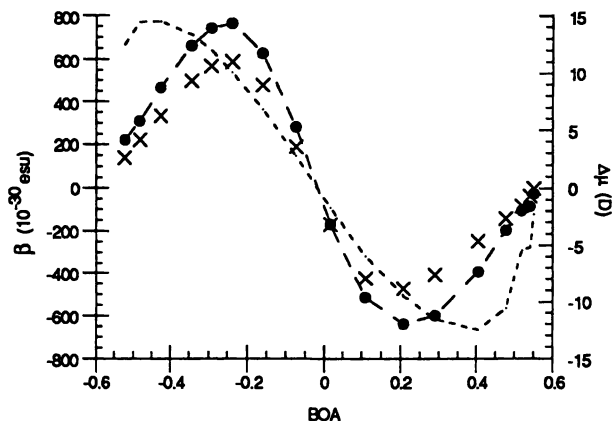

Figure 4. Evolution of: β_{sos} (crosses) and β_{model} (full circles, dashed line) in 10^{-30} esu; $(\mu_{ee}-\mu_{gg})$ (short dashed line) in Debye, plotted vs. BOA.
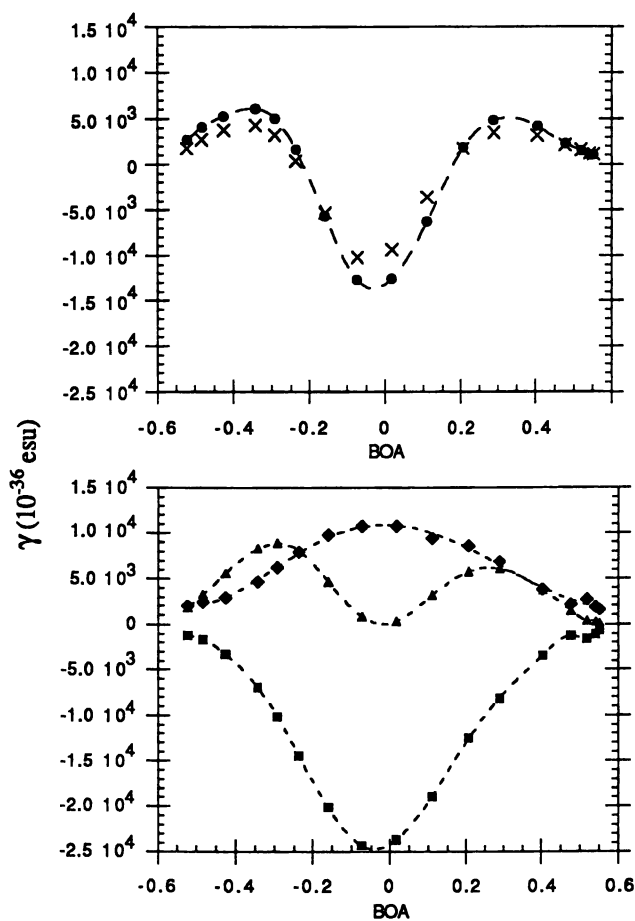
Figure 5. Evolution of: γ_{sos} (crosses) and γ_{model} (full circles, dashed line) [top], and the D-(triangles), N-(squares), and T-terms (diamonds) [bottom] in 10^{-36} esu, plotted vs. *BOA*.

The first hyperpolarizability, β, as a function of increasing ground-state polarization, exhibits a positive peak, a sign change at zero *BOA*, and a negative peak (Figure 4). Again, the two level calculation for β describes well the basic correlation of β and *BOA*, in terms of both peak position and magnitude. Accordingly, the relation between β and *BOA* can be understood in terms of the model expression (eq. 2) in which β model is proportional to α_{model} scaled by a factor of $(\mu_{ee}-\mu_{gg})/E_{ge}$. Thus, the two peaks in the β curve are a result of the form of α and the sign change and peaks in $(\mu_{ee}-\mu_{gg})$ (Figure 3). The position of the β peaks are closer to zero *BOA* than the $(\mu_{ee}-\mu_{gg})$ peaks since both $(1/E_{ge}^2)$ and μ_{ge}^2 peak at zero *BOA*.

The correlation of γ with *BOA* obtained from the converged sum-over-states calculation and the three-term model *(9-12)* also agree quite well. The expression in eq. 3 consists of a negative term, N, proportional to α_{model}^2, a two-photon term, T, and a term, D, proportional to $\beta_{model}^2/\alpha_{model}$. For chromophores with large negative *BOA*, such as unsubstituted polyenes, the D term is negligible due to a small $(\mu_{ee}-\mu_{gg})$ and the T term dominates the N term resulting in positive γ (Figure 5). By increasing the ground-state polarization and thus increasing *BOA*, the D term, like β, starts to increase and hence γ increases. However, increasing the ground-state polarization toward the cyanine-limit also increases |N|, ultimately leading to a decrease in γ. As a result of |N| increasing in this region, the peak in the γ curve occurs at a larger magnitude of *BOA* than the peak in the D term. Upon further polarization, D peaks in a positive sense and starts to decrease and |N| continues to increase and thus γ decreases and goes through zero when |N| = T + D. At the bond-equivalent cyanine-limit the D term is zero since $(\mu_{ee}-\mu_{gg})$ is zero and the γ curve exhibits a negative peak, since both |N| and T peak but |N| > T (Figure 5). To a first approximation, the behavior of γ in the region of positive *BOA* mirrors that in the negative *BOA* region.

Relationships between *BLA* and α, β, and γ in the VB-CT model

The structural evolution of the DA polyenes as calculated by AM-1 or INDO-SDCI methods as a function of a strong static field can qualitatively described in terms of a superposition of valence-bond and charge-transfer resonance structures. We recently developed a simple semiclassical VB-CT model based on such a picture for DA polyenes, to illustrate the dependence of the structural evolution on VB-CT energetics and thereby provide further insight into the structure-hyperpolarizability relationships. In the VB-CT model, *(7)* the mixing of the two resonance forms along a continuous *BLA* coordinate, q, is treated. This mixing results in a ground-state potential surface whose equilibrium value of *BLA* depends on, among other factors, the zero-order adiabatic energy difference, $V_o = E_{CT} - E_{VB}$, and the charge transfer matrix element, t. When V_o is large, the ground state resembles the neutral resonance form, whereas when V_o is negative and large in magnitude, the ground state resembles the charge-transfer resonance form. For intermediate V_o, the structure evolves rapidly, with the greatest rate of change at $V_o = 0$, where the structure is cyanine-like. The value of V_o depends on the donor and acceptor strength and the difference in energy of the bridge in the two states. Additionally, since the two states have a large difference in dipole moment, $\mu_{VB} \sim 0$, $\mu_{CT} \sim e\,R_{DA}$, the application of an electric field or the screening of the charges due to the solvent dielectric response also affects the energy difference.

In order to calculate the structure-property relationships as V_o is varied, we computed the eigenstate potential surfaces (see Figure 6), obtained the equilibrium structure on the ground state potential surface, and then calculated the dipole moment,

polarizability and hyperpolarizabilities, for a given value of V_O. The zero-order potential surfaces were taken to be harmonic in this simple model. The calculation was repeated over a range of V_O, from which we obtained the dependence of the polarization, polarizabilities, and *BLA* on V_O. The ground state wavefunction is written in terms of VB and CT wavefunctions as:

$$\Psi_{gr} = \sqrt{1-f}\,\psi_{VB} + \sqrt{f}\,\psi_{CT} \tag{4}$$

where f is the charge-transfer fraction, $f = 1/2 - V/2(V^2 + 4t^2)^{1/2}$. Here V represents the vertical energy difference between VB and CT harmonic surfaces at a particular q. The ground-state energy (taking E_{VB} ($q = -0.12\text{Å}$) = 0) for the two-state system is:

$$E_{gr} = \frac{1}{2}\left(V - \sqrt{V^2 + 4t^2}\right) \tag{5}$$

To find the equilibrium structure we solved $dE_{gr}/dq = 0$, from which one can show (7) that $q_{eq} = -0.12 + 0.24f$. Thus, *BLA* and the charge transfer fraction are linearly related in this model. The value of q_{eq} for a given value of V_O was found either by a numerical search for the minimum or by solving the equation for q_{eq} iteratively. Recognizing that $\mu = f\mu_{CT}$ and that the polarizabilities are the derivatives of μ with respect to field strength, we obtained analytic expressions for α, β, γ, and δ:

$$\alpha = \frac{2t^2\mu_{CT}^2}{E_g^3} \tag{6}$$

$$\beta = \frac{3t^2\mu_{CT}^3 V}{E_g^5} \tag{7}$$

$$\gamma = \frac{4t^2\mu_{CT}^4(V^2 - t^2)}{E_g^7} \tag{8}$$

$$\delta = \frac{5t^2\mu_{CT}^5 V(V^2 - 3t^2)}{E_g^9} \tag{9}$$

where $E_g = (V^2 + 4t^2)^{1/2} = hc/\lambda_{max}$ is the energy gap. It should be emphasized that V and E_g are the values at q_{eq} for a particular V_O. The relationships between the polarizabilities, as function of static field strength, and the structural evolution have been discussed in earlier papers (3,7).

To a first approximation, molecules of a given length and bridge type can be taken to have the same t and μ_{CT}, thus the polarizabilities and the structure vary primarily due to variations in V_O. Figure 7 shows the calculated dependencies for α, β, and γ as a function of V_O. The calculated dependencies exhibit very similar trends to those discussed above in the context of the molecular orbital calculations. Since E_g is at a minimum (i.e. $E_g = 2t$) when $V_O = 0$, which is where *BLA = 0*, α is peaked, β is zero, and γ is at a negative extreme. With further stabilization of the CT state, whereupon it becomes the lower energy zero-order state, V becomes negative
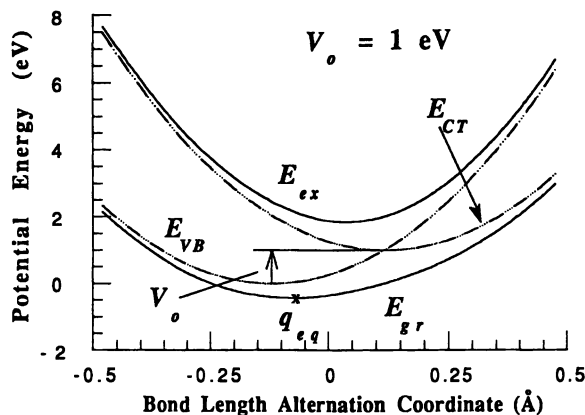
Figure 6. Potential energy surfaces for zero-order VB and CT states, and the ground and excited eigenstates, corresponding to a zero-order adiabatic energy difference of 1 eV. A harmonic force constant of 33.5 eV/Å² was used for the zero-order surfaces and the charge transfer matrix element, t, was taken as 1.18 eV. The equilibrium coordinates for VB and CT are -0.12 Å and 0.12 Å, respectively. The x marks the equilibrium coordinate (q_{eq}) on the ground state potential surface.
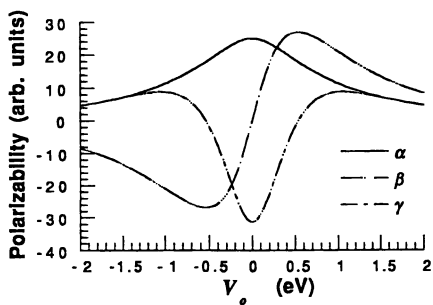

Figure 7. α, β, and γ as a function of V_0 calculated using the VB-CT model for a DA polyene with nine conjugated atoms. The left extreme corresponds to zwitterionic structures and the right side to neutral polyene like structures.

and from eq. 7 so does β. Of course, this sign change is also associated with a change in sign of ($\mu_{ee}-\mu_{gg}$), which was discussed above. The value of β reaches extremes when $V = \pm t$, thus $E_g = \sqrt{5}t$, which is also where $\gamma = 0$. The value of γ reaches maxima when $V = \pm \sqrt{3}t$, whereupon $E_g = \sqrt{7}t$.

While the trends calculated using the VB-CT model agree qualitatively well with the AM-1 and INDO sum-over-states calculations, there are some small differences, particularly in the detailed shape of the γ curve (7). In the sum-over-states calculations, the positive peak value of γ (relative to that of the negative peak) is larger than is found in the valence bond model. In the VB-CT model used here only two states contribute to γ, however, as we have discussed above, there are significant positive contributions from higher lying two-photon states (the T term in eq. 3). We believe that the omission of such terms in the valence bond treatment may lead to these differences. It is possible to develop a more complete valence bond model in which various bridge localized excited states are taken into account. The treatment of such states has been described recently, (8) and its inclusion with the present VB-CT model is being investigated.

Figures 8 and 9 show plots of the $\mu\beta$ product, which is the microscopic quantity relevant to EFISH and poled-polymer electro-optic responses, and γ *versus* λ_{max} for a DA octatetraene calculated using the VB-CT model as V_0 was varied from -2 to 2 eV. These plots illustrate the nonlinearity-transparency trade-off (as measured by λ_{max}) for DA molecules of a fixed length that vary over the domain of *BLA*. The value of $\mu\beta$, Figure 8, reaches a maximum when λ_{max} is about 490 nm (for DA polyenes with nine conjugated atoms) but decreases and goes to zero as λ_{max} reaches its maximum at ~ 520 nm (the so-called cyanine-limit). Thus, structural changes that lead to an increase in λ_{max} at fixed length do not always lead to an increase in $\mu\beta$. The lower arm of the $\mu\beta$ plot corresponds to highly polarized molecules that are dominantly zwitterionic. Since the dipole moment increases as the CT form is stabilized, the negative peak of $\mu\beta$ is substantially larger in magnitude than positive peak. The negative $\mu\beta$ peak occurs near 450 nm, substantially blue shifted relative to the positive peak. This increased nonlinearity and transparency of zwitterionic molecules near the negative extreme of $\mu\beta$ makes such molecules attractive candidates for poled polymer applications.

Because the dependence of γ on V_0 is symmetric about $V_0 = 0$ (Figure 7) the γ versus λ_{max} plot folds back on top of itself as the polarization is increased, giving the simple curve in Figure 9. Accordingly, in contrast to what was calculated for the $\mu\beta$ values, there is no intrinsic advantage to highly zwitterionic DA polyenes for γ. The positive peak of γ occurs near 400 nm but the negative peak, which is several times larger in magnitude, occurs when λ_{max} is at its maximum of 520 nm (the cyanine limit). With their large negative γ values, cyanines or DA molecules at the cyanine limit could be of interest for self-defocusing applications (like optical power limiting), or for the engineering of materials with vanishing third-order nonlinearity, through the destructive interference of the negative contribution of the cyanine and the positive nonlinearity of a host medium.

It is not uncommon to find in the literature fits of $\mu\beta$ and γ to power laws in λ_{max}. In view of the dependencies in Figures 8 and 9, it can been seen that for DA polyenes at a fixed length, a simple power law relation is not obeyed over the domain of structural variation. For DA polyenes varying in length considerable caution is needed in interpreting power law fits in length or in λ_{max}. This is because the degree of polarization and the *BLA* of the molecules could be length dependent.
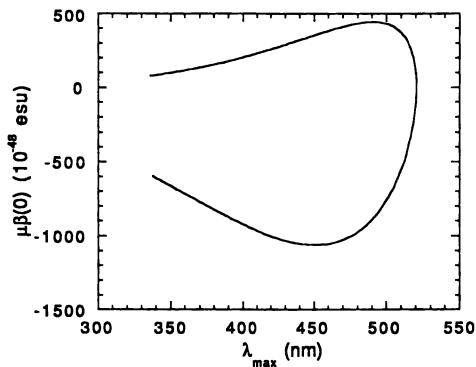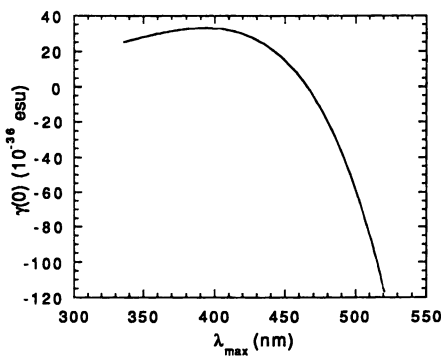
Figure 8. Dependence of $\mu\beta(0)$ on λ_{max} for a DA polyene of nine conjugated atoms calculated using the VB-CT model. The calculations were performed using the following parameters: harmonic force constant, $k = 33.55$ eV/Å^2, $R_{DA} = 7.3$ Å, $t = 1.18$ eV, and the charge transfer efficiency, $Q = 0.5$ ($\mu_{CT} = Q$ |e| R_{DA}).

Figure 9. Dependence of $\gamma(0)$ on λ_{max} for a DA polyene of nine conjugated atoms calculated using the VB-CT model. The calculations were performed using the same parameters as for Figure 8.

Conclusions

For simple DA polyene dyes, α, β, and γ can be correlated with either *BLA* or *BOA* as demonstrated using semi-empirical INDO/SDCI calculations. The trends obtained through these calculations are in qualitative agreement with a simple model based on VB and CT mixing that involves harmonic potentials for the zero-order states. This model provides a simple physical picture for the evolution of the structure of DA polyenes as the CT state is stabilized. In this model, analytical dependencies of the polarization and polarizabilities on the energetics and interaction of VB and CT states are obtained, although the equilibrium structure must be found numerically. The agreement obtained between the different levels of theory (AM-1, INDO-SDCI, and VB-CT model) suggests that the trends obtained are robust and, therefore, provide useful guidelines for the design of optimized molecules for nonlinear optics.

Acknowledgments

Literature Cited

1. Marder, S. R.; Perry, J. W.; Bourhill, G.; Gorman, C. B.; Tiemann, B. G.; Mansour, K. *Science* **1993**, *261*, 186.
2 Bourhill, G.; Brédas, J.-L.; Cheng, L.-T.; Marder, S. R.; Meyers, F.; Perry, J. W.; Tiemann, B. G. *J. Am. Chem. Soc.* **1994**, *116*, 2619.
3. Marder, S. R.; Gorman, C. B.; Meyers, F.; Perry, J. W.; Bourhill, G.; Brédas, J.-L.; Pierce, B. M. *Science*, **1994**, *265*, 632.
4. Gorman, C. B.; Marder, S. R. *Proc. Natl. Acad. Sci. USA* **1993**, *90*, 11297.
5. Meyers, F.; Marder, S. R.; Pierce, B. M.; Brédas, J.-L. *Chem. Phys. Lett.*, **1994**, *228*, 171.
6. Meyers, F.; Marder, S. R.; Pierce, B. M.; Brédas, J.-L. *J. Am. Chem. Soc.*, **1994**, *116*, 10703.
7. Lu, D.; Chen, G.; Goddard, III, W. A.; Perry, J. W. *J. Am. Chem. Soc.*, **1994**, *116*, 10679.
8. Lu, D.; Chen, G.; Goddard, III, W. A., *J. Chem. Phys.*, **1994**, *101*, 5860.
9. Kuzyk, M. G.; Dirk, C. W., *Phys. Rev. A* **1990**, *41*, 5098.
10. Dirk, C. W.; Cheng, L. T.; Kuzyk, M. G. *Int. J. Quantum Chem.* **1992**, *43*, 27.

11. Garito, A. F.; Heflin, J. R.; Wong, K. Y.; Zamani-Khamiri, O., in *Organic Materials for Nonlinear Optics*; Hann, R. A., Bloor, D., Eds. Royal Soc. Chem. **1989**, 16.
12. Pierce, B. M., Proc. *SPIE-Int. Soc. Opt. Eng.* **1991**, *1560*, 148.